

## **Thermodynamic performance analysis and flammability study of various new ozone friendly non azeotropic refrigerant mixtures as alternatives to replace R22 used in residential air conditioners**

Sharmas Vali Shaik\*, Talanki Puttaranga Ashok Babu

Department of Mechanical Engineering, National Institute of Technology Karnataka, NITK Surathkal-575025, Mangalore, India

Corresponding Author Email: [sharmasvali.nitk@gmail.com](mailto:sharmasvali.nitk@gmail.com)

<https://doi.org/10.18280/ijht.360441>

### **ABSTRACT**

**Received:** 28 February 2018

**Accepted:** 8 October 2018

#### **Keywords:**

*COP, flammability, GWP, power savings, R22 alternatives, R32/R134a/R1270 blend*

The present study investigates the theoretical thermodynamic performance analysis and flammability study of various new ozone friendly refrigerants as replacements to R22. In this work, five non azeotropic refrigerant blends comprising of R152a, R134a, R32, R290 and R1270, at various compositions were developed. Flammability study of all the five refrigerant mixtures considered were carried out by using Refrigerant Flammability (RF) number. The cycle followed during the performance investigation of refrigerants was the actual vapour compression refrigeration cycle. Thermodynamic performance characteristics of all the five investigated refrigerants were compared with the baseline refrigerant R22. Theoretical results showed that COP of refrigerant M40 was 0.51% higher, compared to R22 and the five refrigerants studied. Compressor discharge temperature of M40 was lowered by 11.6°C compared to R22. Power consumed to produce per ton of refrigeration of M40 was 0.52% lower, compared to R22 and the five refrigerants considered. Heat transfer rate through the condenser for M40 was 3.66% higher than R22. Volumetric refrigeration capacity of M40 was the highest among the five studied refrigerants and it was very close to the volumetric capacity of R22. Flammability analysis revealed that all the five investigated refrigerant mixtures were classified into the weakly flammable category. Overall, the thermodynamic performance of new ternary blend M40 (R32/R134a/R1270 5/60/35 by mass percentage) was higher than R22 with reasonable saving in power consumption and hence, M40 is a viable candidate to replace R22.

## **1. INTRODUCTION**

Due to adverse ecological effects of Hydrochlorofluorocarbon (HCFC) refrigerant R22, Montreal protocol has been decided to phase out all the HCFCs by the year 2030, since HCFCs contain high global warming potential (GWP) and ozone depleting potential (ODP) [1-2]. In this context, many developing and developed countries have spent much effort to develop their own alternative refrigerants to replace R22. In the past several years, performance studies on various refrigerants were carried out to recommend the alternatives to R22.

Investigational studies suggested that R407C was an appropriate retrofit refrigerant to R22 [3]. Performance investigation of ternary blend consisting of R744/R32/R134a (7/31/62 by mass %) was carried out on heat pump experimentally, to replace R22 [4]. Test results revealed that COP of above blend was 2.5% higher than R22. This ternary blend was suitable for low temperature heat pumps due to its surplus condensing temperature. Experimental investigations showed that ternary blend consisting of R125/R32/R161 (34/15/51 by wt %) was a favorable refrigerant substitute for R407C [5]. Theoretical thermodynamic analysis was carried out in a variable refrigerant flow system with R32 as a replacement candidate to R410A [6]. Results revealed that COP of R32 was 5-6% higher than R410A, under the mode of heating and cooling conditions, respectively.

Performance studies of two binary blends like R32/R134a (26/74 by mass %) and R32/R134a (30/70 by mass %) were conducted in a heat pump tester [7]. Test results showed that, performance of the above two mixtures was greater compared to base line refrigerant R22. Experimental studies were carried out in a heat pump with RE170, R1270, R290, R152a and its various blends as alternatives for R22 [8]. Test results showed that COP of all the studied fluids was better than the baseline refrigerant R22. Experiments were done in an air conditioner with two R22 retrofit refrigerants like R404A and R507 [9]. Test results exhibited that R507 performs better than R22 and R404A. Experimental tests were carried out with R431A in a heat pump apparatus, working under the mode of both air conditioning and heat pump conditions [10]. Results showed that performance of R431A was 3.5 to 3.8% greater compared to base line refrigerant R22.

Experimental studies reported that R407C performs better than R417A and R507A [11]. Experimental tests were conducted to measure the heat pump device performance using R600, R600a, R290, R1270 and two binary blends such as R290/R600 and R290/R600a [12]. Experimental test results showed that the performance of both R290 and R1270 was superior compared to the reference fluid R22. The present study concentrates on thermodynamic performance as well as flammability analysis of five ozone friendly, low, GWP non azeotropic refrigerant blends as alternatives to R22.

The performance characteristics of refrigerants are also computed for various evaporator temperatures by keeping the condenser temperature constant.

## 2. ALTERNATIVE REFRIGERANTS AND THEIR PROPERTIES

In the present study apart from R407C, five alternative refrigerant mixtures comprising of R32, R134a, R152a, R290 and R1270, at various composition were developed. Designation of refrigerants which were developed in this study are shown in Table 1. Similarly basic properties of alternative refrigerants are shown in Table 2.

**Table 1.** Designation of investigated alternative refrigerants

Designation of refrigerants	Composition (mass %)
R22	Pure fluid
M10 (R32/R134a)	26/74
M20 (R32/R134a)	30/70
M30 (R32/R134a/R152a)	17.5/65/17.5
M40 (R32/R134a/R1270)	5/60/35
M50 (R32/R134a/R290)	5/60/35
R407C (R32/R125/R134a)	23/25/52

**Table 2.** Properties of alternative refrigerants

Refrigerants	MW (kg/kmol)	BP (°C)	T <sub>bub</sub> (°C)	T <sub>dew</sub> (°C)	T* <sub>glide</sub> (°C)
R22	86.5	-40.81	0	0	0
M10	81.631	-	-40.49	-33.46	7.03
M20	79.194	-	-41.68	-34.51	7.17
M30	80.75	-	-36.37	-29.57	6.80
M40	65.967	-	-50.62	-42.18	8.44
M50	67.664	-	-49.49	-42.77	6.72
R407C	86.204	-	-43.63	-36.63	7.0

T\*<sub>glide</sub> = (T<sub>dew</sub> - T<sub>bub</sub>) at 0.101325MPa

**Table 2.** Continued

Refrigerants	T <sub>c</sub> (K)	P <sub>c</sub> (MPa)	ODP	GWP (100 years)
R22	369.3	4.990	0.055	1760
M10	365.83	4.776	0	1138
M20	364.73	4.858	0	1113
M30	371.68	4.659	0	988
M40	355.15	4.356	0	815
M50	351.81	4.086	0	815
R407C	359.29	4.639	0	1774

From Table 2, it is observed that all the five refrigerant blends are non azeotropic. This is due to their higher temperature glide. All the developed refrigerants are ozone friendly and have low GWP compared to base line refrigerant R22. In this investigation, Martin-Hou equation of state was used to develop the thermodynamic properties of all the investigated blends which are essential for thermodynamic analysis [13].

The significance of Martin-Hou equation of state is that, it gives the better accuracy and results for the estimation of thermodynamic properties of pure and mixture refrigerants [13-15]. The properties of refrigerants like R407C and R22, matches well with the ASHRAE refrigerants experimental properties data hand book [16]. The percentage variation in the estimated properties of R407C and R22 compared with ASHRAE was within 2% for the given operating conditions.

Hence, the procedure followed to develop the properties of R407C and R22 is considered as reliable. Therefore, same methodology is followed to develop the thermodynamic properties of new refrigerants as well.

## 2.1 Procedure to develop thermodynamic properties of pure and mixture refrigerants

Procedure followed for the development of properties of refrigerants was taken from literature and it is explained below [17-18].

### 2.1.1 Procedure for pure refrigerants

Various correlations used to establish the thermodynamic properties of refrigerants are given in this section. P-h chart used while developing the properties of pure refrigerants is shown in Figure 1. Step by step procedure followed to develop the properties of refrigerants is given below.

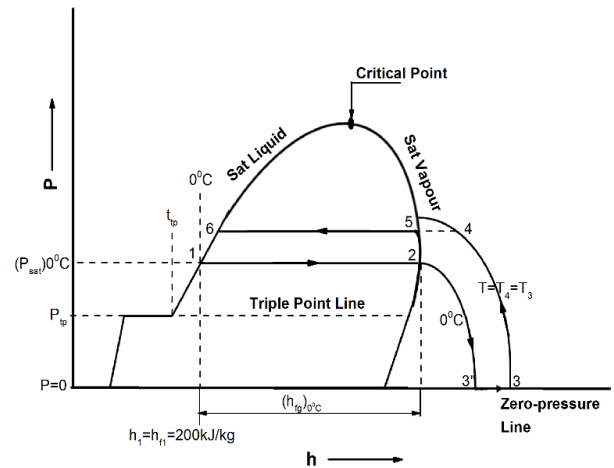


**Figure 1.** P-h diagram for computing the properties of pure refrigerant

First of all find the saturation pressure of the given refrigerant. The correlation between saturation pressure (P<sub>sat</sub>) and saturation temperature (T<sub>sat</sub>) was given by Wagner equation and it is given below [19].

$$\ln\left(\frac{P_{sat}}{P_c}\right) = \left(\frac{1}{1-x}\right) [Ax + Bx^{1.5} + Cx^{2.5} + Dx^5] \quad (1)$$

where  $x=1-T/T_c$ ; A, B, C and D are constants for a particular refrigerant. The above constants for various refrigerants were available in literature [19]. For example, saturation vapour pressure constants for refrigerant R22 are shown in Table 3.

**Table 3.** Constants of R22 for equation (1)

A	B	C	D
-7.0682	1.52369	-1.8545	-2.8439

Find the liquid density of given refrigerant. In this study, Reid et al. correlation was used to find the liquid density of various refrigerants [20-21].

$$\rho_r = \frac{\rho}{\rho_c} = 1 + 0.85 \times (1 - T_r) + (1.6916 + 0.984 \times \omega) \times (1 - T_r)^{1/3} \quad (2)$$

where  $\omega$  is acentric factor;  $T_r=T/T_c$ ,  $\omega$ ,  $\rho_c$  and  $T_c$  are constants

for the various refrigerants. These constants for the various refrigerants were available in literature [18]. For example, constants of R22 for equation (2) are given in Table 4.

**Table 4.** Constants of R22 for equation (2)

$\omega$	$\rho_c$ (kg/m <sup>3</sup> )	$T_c$ (K)
0.221	523.8	369.15

Find the specific volume of vapour refrigerant. In this study, specific volume of vapour for all the refrigerants considered is computed by using Martin-Hou equation of state (MHEOS) [13].

$$P = \frac{RT}{V-b} + \frac{A_2+B_2T+C_2e^{-\frac{5.475T}{T_c}}}{(V-b)^2} + \frac{A_3+B_3T+C_3e^{-\frac{5.475T}{T_c}}}{(V-b)^3} + \frac{A_4}{(V-b)^4} + \frac{B_5T}{(V-b)^5} \quad (3)$$

where  $A_2, A_3, A_4, B_2, B_3, B_5, C_2, C_3$  and  $b$  are the dimensionless coefficients of Martin-Hou equation of state (MHEOS) for the various refrigerants. Procedure followed to compute the above coefficients was explained in the literature [13]. By solving the above equation (3), the dimensionless coefficients for R22 are listed in Table 5.

**Table 5.** Dimensionless coefficients of Martin-Hou equation of state for R22

Dimensionless coefficients of MHEOS for R22	Values
$A_2$	-139.154038231457
$A_3$	0.295289024195263
$A_4$	-0.000104165697806786
$B_2$	0.128645931301646
$B_3$	-0.000446322328392750
$B_5$	8.14900447033360×10 <sup>-11</sup>
$C_2$	-2292.28498497122
$C_3$	3.44337587584321
$b$	0.000407841281333333

Compute the enthalpy of vapourization of various refrigerants by using Clausius-Clapeyron equation.

$$\frac{dP_{sat}}{dT} = \frac{h_{fg}}{T \times V_{fg}} \quad (4)$$

where  $V_{fg} = v_g - v_f$

Apply the departure method to find the enthalpy and entropy of various refrigerants [17-18]. While computing the properties, the reference state for enthalpy and entropy is to be fixed. In case of refrigerants, values of enthalpy and entropy assigned to the reference state of saturated liquid at 0°C are  $h_1=h_{fl}=200$  kJ/kg and  $S_1=S_{fl}=1.0$  kJ/kg K respectively [17-18].

The significance of departure function is, to compute the enthalpy and entropy at various points as shown in Figure 1 (P-h diagram). To compute the enthalpy at point 3, the enthalpy departure method is used. The enthalpy departure term ( $h_3-h_2$ ) is given as follows.

$$h_3 - h_2 = (U_3 - U_2) + (P_3V_3 - P_2V_2) \quad (5)$$

$$U_3 - U_2 = \int_2^3 \left[ T \left[ \frac{\partial P}{\partial T} \right]_V - P \right] dV \quad (6)$$

By solving the equations (5) and (6) the value of  $h_3$  can be found. In order to find the enthalpy  $h_4$  at point 4, ideal gas heat capacity correlation and enthalpy difference ( $h_4-h_3$ ) can be used and it is given below.

$$h_4 - h_3 = \int_3^4 C_{P0} dT \quad (7)$$

In the present work, ideal gas heat capacity ( $C_{P0}$ ) correlation was taken from the literature and it is given below [18].

$$C_{P0} = G_0 + G_1T + G_2T^2 + G_3T^3 + G_4T^4 \quad (8)$$

where  $G_0, G_1, G_2, G_3$  and  $G_4$  are the constants for various refrigerants. The above constants for various refrigerants were available in the literature [18]. For example, constants of ideal gas heat capacity correlation for R22 are shown in Table 6.

**Table 6.** Constants of R22 for equation (8)

$G_0$	$G_1$	$G_2$	$G_3$	$G_4$
2.55513	17.1926	-0.890386	-0.10517	0.146405
	×10 <sup>-3</sup>	×10 <sup>-5</sup>	×10 <sup>-8</sup>	×10 <sup>-11</sup>

Again enthalpy departure term is used in between the state points 4 and 5 in order to find enthalpy  $h_5$ .

$$h_5 - h_4 = (U_5 - U_4) + (P_5V_5 - P_4V_4) \quad (9)$$

$$U_5 - U_4 = \int_4^5 \left[ T \left[ \frac{\partial P}{\partial T} \right]_V - P \right] dV \quad (10)$$

By solving the above equations (9) and (10) the value of  $h_5$  can be found. The saturated liquid enthalpy at state point 6 can be found by using the following relation.

$$h_5 - h_6 = h_{fg} \quad (11)$$

$$h_6 = h_5 - h_{fg} \quad (12)$$

where  $h_{fg}$  is found by using Clausius-Clapeyron equation at a given temperature.

Find the liquid entropy of given refrigerant. To compute the thermodynamic properties (enthalpy and entropy) of refrigerant at any given pressure and temperature, the departure method is used and the corresponding saturated liquid enthalpy and saturated liquid entropy is calculated by using the Clausius-Clapeyron equation. Entropy of liquid for the given refrigerant can be calculated as follows.

$$S_{fg} = S_g - S_f \quad (13)$$

$$S_f = S_g - S_{fg} \quad (14)$$

Find the vapour entropy of refrigerant. Entropy of vapour for the given refrigerant can be computed as follows.

$$S_{fg} = \frac{h_{fg}}{T_{sat}} \quad (15)$$

$$S_g = \frac{h_g}{T_{sat}} \quad (16)$$

By following the above methodology, thermodynamic properties of various pure refrigerants can be found. Similarly procedure followed to compute the thermodynamic properties of refrigerant mixtures is given below.

### 2.1.2 Procedure for refrigerant mixtures

P-h chart used while developing the properties of refrigerant mixtures is shown in Figure 2.

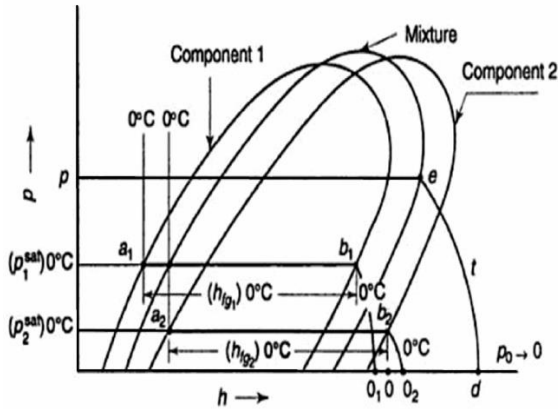


**Figure 2.** P-h diagram for computing the properties of refrigerant mixtures

(i) To develop the properties of refrigerant mixtures, the properties of pure refrigerants data were taken into account.

(ii) Bubble point temperature and dew point temperature of refrigerant mixtures are computed by using the interpolation method and by taking the saturation temperature and pressure data of pure refrigerants [17].

(iii) Mixing rules and binary interaction parameter used while developing and establishing the thermodynamic properties of refrigerant mixtures were taken from the literature [18, 22]. These rules are used to find critical temperature and critical pressure of the refrigerant mixture.

$$T_{cm} = y_i^2 T_i + y_j^2 T_j + 2y_i y_j T_{cij} \quad (17)$$

$$T_{cij} = (1 - k_{ij})(T_{ci} T_{cj})^{1/2} \quad (18)$$

$$1 - k_{ij} = \frac{8(V_{ci} V_{cj})^{1/2}}{(V_{ci}^{1/3} + V_{cj}^{1/3})^3} \quad (19)$$

$$P_{cm} = \frac{(Z_{cm} R T_{cm})}{(V_{cm})} = \frac{((\sum_{i=1}^n y_i Z_{ci})(R)(\sum_{i=1}^n y_i T_{ci}))}{(\sum_{i=1}^n y_i V_{ci})} \quad (20)$$

The binary interaction parameter  $k_{ij}$  is given by

$$k_{ij} = 1 - \frac{8(V_{ci} V_{cj})^{1/2}}{(V_{ci}^{1/3} + V_{cj}^{1/3})^3} \quad (21)$$

(iv) Specific volume of vapour for the given refrigerant mixture can be computed by using Martin-Hou equation of state.

(v) Similarly departure method is used to find the enthalpy and entropy of various refrigerant mixtures and the procedure for departure method was explained in the literature [17-18].

By following the above methodology, thermodynamic properties of various refrigerant mixtures can be found. The computed thermodynamic properties of refrigerants like

R407C and R22, matches well with the ASHRAE refrigerants experimental properties data hand book [16]. Deviation of computed properties of R407C and R22 compared with ASHRAE was within 2% for the given operating conditions. Therefore, the methodology followed to compute the properties of R407C and R22 is reliable. Hence, same methodology is followed to develop the thermodynamic properties of new refrigerants as well, since thermodynamic properties of new refrigerants are not available in the literature.

### 3. FLAMMABILITY STUDY

Study of flammability is very essential for the researchers while developing alternative refrigerants. ASHRAE safety standard 34 reveals that, flammability of refrigerants is categorized into various safety groups like non-flammable (A1), weakly flammable (A2) and highly flammable (A3) groups respectively [23]. From this safety standard, it is found that, refrigerants R22, R134a, R125 and R407C are classified into non-flammable group (A1) whereas R32 and R152a are classified into weakly flammable (A2) respectively. Similarly R290 and R1270 are classified into highly flammable (A3).

However flammability group of various new mixture refrigerants (M10, M20, M30, M40, and M50) are not available in the ASHRAE safety standard 34, hence refrigerant flammability number (RF number) was used in this study for assessing the flammability of new mixture refrigerants. RF number has good agreement with that of ASHRAE safety standard 34 which is used for classifying the refrigerants into various flammability groups [24]. It is reliable to express the hazards of combustion with respect to limits of flammability of each refrigerant by using refrigerant flammability (RF) number. Depending upon RF number, refrigerants are classified into various categories [24]. If RF number is less than 30 kJ/g, then they are categorized as weakly flammable refrigerants (ASHRAE A2) and if it is in between 30 to 150 kJ/g, then they are classified as highly flammable refrigerants (ASHRAE A3). An empirical correlation used for calculating the RF number of the five refrigerants studied, is given below.

$$RF \text{ number} = \left[ \left( \frac{UFL}{LFL} \right)^{0.5} - 1 \right] \frac{q}{MW} \quad (22)$$

By using the above formula the values of RF number of various new refrigerant mixtures (M10, M20, M30, M40 and M50) were calculated and they are shown in Table 7. Similarly the summary of flammability groups of all the R22 alternatives investigated in this study are given in the Table 8.

**Table 7.** RF number and flammability group of refrigerants

Refrigerants	RF number (kJ/g)	ASHRAE flammability group
M10	9.13	A2*
M20	8.88	A2*
M30	10.00	A2*
M40	18.19	A2*
M50	18.14	A2*

\* Estimated values of RF number

From the Table 7 it is found that, flammability of all the five investigated refrigerants (M10 to M50) are categorized into weakly flammable group (ASHRAE A2), because RF number of these refrigerants was below 30 kJ/g.

**Table 8.** ASHRAE safety group of various R22 alternative refrigerants

Refrigerants	ASHRAE safety group	ASHRAE flammability
R22	A1	A1 Non flammable
R134a	A1	A1 Non flammable
R125	A1	A1 Non flammable
R32	A2	A2 Weakly flammable
R152a	A2	A2 Weakly flammable
R290	A3	A3 Highly flammable
R1270	A3	A3 Highly flammable
M10	A2*	A2* Weakly flammable
M20	A2*	A2* Weakly flammable
M30	A2*	A2* Weakly flammable
M40	A2*	A2* Weakly flammable
M50	A2*	A2* Weakly flammable
R407C	A1	A1 Non flammable

\*Estimated

#### 4. VAPOUR COMPRESSION REFRIGERATION SYSTEM

The schematic representation of vapour compression refrigeration (VCR) system is shown in Figure 3 [17]. Residential air conditioners work on the principle of vapour compression refrigeration system.

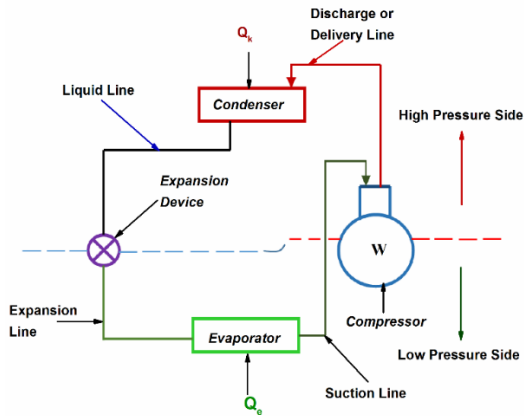


**Figure 3.** Schematic diagram of vapour compression refrigeration system

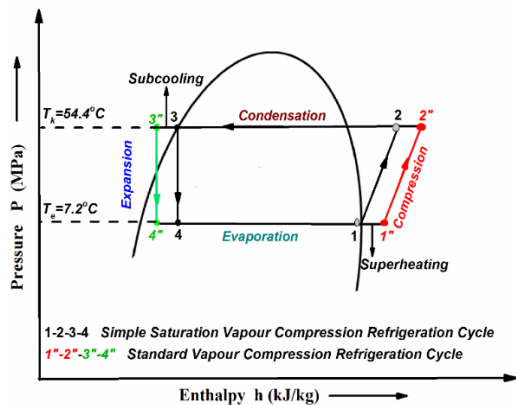


**Figure 4.** P-h diagram of standard vapour compression cycle

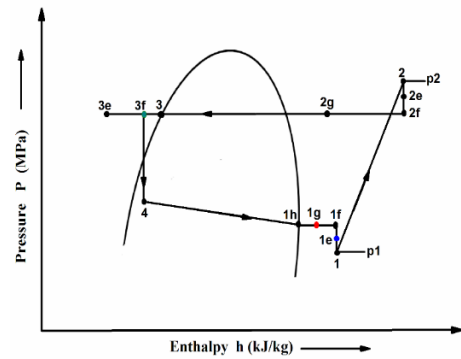


**Figure 5.** P-h diagram of actual vapour compression cycle

In majority of literature, thermodynamic analysis of air conditioners was done based on either simple saturation or standard vapour compression cycle [25-28]. The P-h diagram of standard vapour compression cycle is shown in Figure 4. In this standard cycle, pressure losses and heat losses to the surroundings from condensers and evaporators are neglected. Similarly suction line pressure drop, discharge line pressure drop and heat gain or heat losses occur at various device of the system are neglected for the ease of theoretical computations.

However in actual practice, subcooling, superheating, pressure losses and heat gain or heat losses occur at various system components. All the above losses are considered in the actual vapour compression cycle. Hence, the present study considered the actual vapour compression refrigeration cycle for the thermodynamic performance analysis of air conditioner. P-h diagram of actual vapour compression cycle is shown in Figure 5. The capacity of air conditioner is taken as 1.5 ton of refrigeration. The description of various state points of the standard vapour compression cycle is shown in Table 9. Similarly description of different state points of actual vapour compression cycle is shown in Table 10.

**Table 9.** Description of standard vapour compression cycle

State points of the cycle	Description
1''-2''	Isentropic compression
2''-3''	Constant pressure condensation
3''-4''	Isenthalpic expansion
4''-1''	Constant pressure evaporation
1-1''	Degree of superheating
3-3''	Degree of subcooling

**Table 10.** Description of actual vapour compression cycle

State points of the cycle	Description
4-1h	Evaporator pressure drop
1h-1g	Superheating of refrigerant in the evaporator
1g-1f	Refrigerant superheating and heat gain in the suction line
1f-1e	Suction line pressure drop
1e-1	Suction valve pressure drop
1-2	Polytropic compression work
2-2e	discharge valve pressure drop
2e-2f	Pressure drop in the discharge line
2f-2g	Desuperheating of refrigerant and heat loss through discharge line
2g-3	Condenser pressure drop
3-3e	Refrigerant subcooling in the condenser
3e-3f	Heat gain through the liquid line

The pressure losses, heat losses and gains occurred at various state points of actual vapour compression cycle are taken from the available literature and they are listed in Table 11 [17, 29].

**Table 11.** Losses considered in the actual vapour compression cycle

Description	Values
Pressure drop in the suction valve	0.2 bar
Pressure drop in the discharge valve	0.4 bar
Pressure drop in the suction line	0.1 bar
Pressure drop in the discharge line	0.1 bar
Pressure drop through evaporator	0.1 bar
Heat gain at inlet of compressor due to temperature rise	10°C
Heat loss at exit of compressor due to temperature drop	10°C
Rise in temperature at expansion valve	2°C
Degree of superheating	11.1°C
Degree of subcooling	8.3°C

## 5. COMPUTATIONAL THERMODYNAMIC PERFORMANCE ANALYSIS

Thermodynamic analysis was carried out to find a suitable alternative to R22. Performance characteristics of R22 and its considered alternatives were evaluated at AHRI conditions and these conditions are shown in Table 12. Actually, AHRI conditions are used in the performance calculation of air conditioners. In this study, thermodynamic analysis of various R22 alternatives was done for both the standard vapour compression cycle and actual vapour compression cycle (Complex cycle).

**Table 12.** AHRI conditions for air conditioners

Operating conditions	Temperature (°C)
Evaporator temperature	7.2
Condenser temperature	54.4
Superheating	11.1
Subcooling	8.3

### 5.1 Thermodynamic performance computations for standard vapour compression refrigeration cycle

Mathematical calculations involved in the performance evaluation of standard vapour compression cycle are given below.

Mass flow rate of refrigerant is computed as

$$\dot{m} = \frac{Q_c}{RE} \quad (23)$$

Refrigerating effect occurred in the evaporator is given by

$$RE = (h_{1''} - h_{4''}) \quad (24)$$

Specific work of compressor is determined by

$$W_c = (h_{2''} - h_{1''}) \quad (25)$$

Coefficient of performance (COP) is computed as

$$COP = RE/W_c \quad (26)$$

Condenser heat rejection (CHR) is given by

$$CHR = (h_{2''} - h_{3''}) \quad (27)$$

Power required per ton of refrigeration (PPTR) is expressed as unit power consumption and it is given by

$$\dot{m} = \frac{Q_c}{RE} = \frac{3.5167}{RE}$$

$$PPTR = \dot{m}W_c = 3.5167 \left( \frac{h_{2''} - h_{1''}}{h_{1''} - h_{4''}} \right)$$

$$PPTR = \dot{m}W_c = 3.5167 \left( \frac{W_c}{RE} \right) = \left( \frac{3.5167}{COP} \right) \quad (28)$$

where  $Q_c$  is capacity of system in ton of refrigeration (TR). Generally 1TR=211 kJ/min = 3.5167 Kw.

Volumetric refrigeration capacity is computed by

$$VRC = \rho_{1''} \times RE = \rho_{1''} \times (h_{1''} - h_{4''}) \quad (29)$$

Heat transfer rate through the condenser is computed as

$$Q_k = \dot{m}(h_{2''} - h_{3''}) \quad (30)$$

Pressure ratio is computed by

$$P_r = \left( \frac{P_k}{P_e} \right) \quad (31)$$

Discharge temperature of compressor ( $T_d$ ) can be found with the help of refrigerants superheated properties Tables and by interpolating for the given superheating value equivalent to difference in entropy, which is known.

Summary of results obtained from this standard vapour compression cycle are given in Table 13.

### 5.2 Thermodynamic performance computations for actual vapour compression refrigeration cycle

Mathematical calculations involved in the performance evaluation of actual vapour compression cycle are given below.

Mass flow rate of refrigerant is computed as

$$\dot{m} = \frac{Q_c}{RE} \quad (32)$$

Refrigerating effect occurred in the evaporator is given by

$$RE = (h_{1g} - h_4) \quad (33)$$

Specific work of compressor is determined by

$$W_c = (h_2 - h_1) \quad (34)$$

Coefficient of performance (COP) is computed as

$$COP = RE/W_c \quad (35)$$

Condenser heat rejection (CHR) is given by

$$CHR = (h_{2f} - h_{3e}) \quad (36)$$

Power required per ton of refrigeration (PPTR) is given by

$$PPTR = \dot{m}W_c = 3.5167 \left(\frac{W_c}{RE}\right) = \left(\frac{3.5167}{COP}\right) \quad (37)$$

Volumetric refrigeration capacity is computed by

$$VRC = \rho_{1g} \times RE = \rho_{1g} \times (h_{1g} - h_4) \quad (38)$$

Heat transfer rate through the condenser is computed as

$$Q_k = \dot{m}(h_{2f} - h_{3e}) \quad (39)$$

Pressure ratio is computed by

$$P_r = \left(\frac{P_k}{P_e}\right) \quad (40)$$

Discharge temperature of compressor ( $T_d$ ) can be found with the help of refrigerants superheated properties Tables and by interpolating for the given superheating value equivalent to difference in entropy, which is known.

Summary of results obtained from this actual vapour compression cycle are given in Table 14.

### 5.3 Validation of results

In this work, a MATLAB program was developed to evaluate the thermodynamic performance characteristics of various considered R22 alternatives. The results obtained from the MATLAB program were compared with the Qiqi

Tian et al. results available in the literature [30]. Qiqi Tian et al. computed the performance characteristics of binary blend R290/R32 (32/68 by wt %) at condenser and evaporator temperatures of 54.4°C ( $T_k$ ) and 7.2°C ( $T_e$ ) respectively, by taking subcooling and superheating as 5°C. For validation, same fluid and operating conditions were used in the program as that of Qiqi Tian et al. The deviation of program results when compared with Qiqi Tian et al. is below 2% and it is shown in Table 15. Hence, the program which is developed in this study is reliable and thus it can be employed for the thermodynamic analysis of various alternative refrigerants considered for the study.

From Tables 13 and 14 it is found that the performance of actual vapour compression system using various R22 alternatives is lower when compared with the performance of standard vapour compression cycle. This is due to various losses occur in the actual cycle which tends to decrease the performance of the system.

**Table 15.** Comparison of performance characteristics of R290/R32 (32/68 by wt %) with Qiqi Tian et al. results

S.no	Performance parameters	Qiqi Tian et al. Results [30]	Program results	Deviation (%)
1	$P_k$ (MPa)	4.027	4.0431	-0.39
2	$P_e$ (MPa)	1.2943	1.2943	0
3	$P_r$	3.11133	3.1237	-0.39
4	RE (kJ/kg)	175.82	173.2102	1.48
5	$W_c$ (kJ/kg)	44.94	45.0741	-0.29
6	COP	3.91	3.8428	1.71
7	$W_{cp}$ (W)	817.93	832.8	-1.81
8	VRC (kJ/m <sup>3</sup> )	5989.439	5884.0	1.76

**Table 13.** Summary of results of performance parameters of various R22 alternatives for standard vapour compression cycle

Refrigerants	$\dot{m}$ (kg/s)	RE (kJ/kg)	$W_c$ (kJ/kg)	COP	Change in COP (%)	$P_k$ (MPa)	$P_e$ (MPa)	$P_r$	$T_d$ (°C)	PPTR (kW/TR)	VRC (kJ/m <sup>3</sup> )	CHR (kJ/kg)	$Q_k$ (kW)
R22	0.03562	148.086	35.718	4.145	0	2.1509	0.6270	3.430	84.26	0.848	3729	183.805	6.547
M10	0.03193	165.185	47.629	3.468	-16.33	2.2868	0.5082	4.499	85.74	1.013	3130	212.815	6.795
M20	0.03121	168.998	49.132	3.439	-17.03	2.3842	0.5301	4.497	87.43	1.022	3232	218.130	6.808
M30	0.02893	182.314	48.526	3.757	-9.36	1.9810	0.4432	4.469	82.91	0.936	2918	230.840	6.679
M40	0.02441	216.054	50.418	4.285	3.37	2.0274	0.5398	3.755	72.74	0.820	3531	266.472	6.505
M50	0.02612	201.890	49.071	4.114	-0.747	1.8226	0.4924	3.701	71.87	0.854	3114	250.961	6.557
R407C	0.03530	149.393	44.172	3.382	-18.40	2.4731	0.5711	4.330	83.97	1.039	3334	193.566	6.834

**Table 14.** Summary of results of performance parameters of various R22 alternatives for actual vapour compression cycle

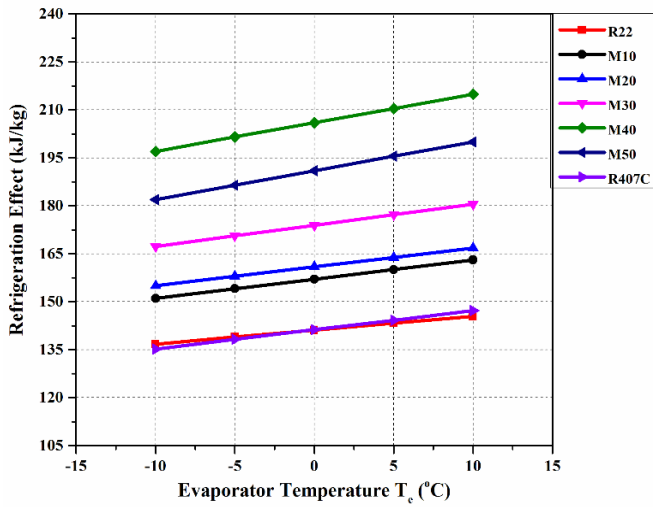
Refrigerants	$\dot{m}$ (kg/s)	RE (kJ/kg)	$W_c$ (kJ/kg)	COP	Change in COP (%)	$P_k$ (MPa)	$P_e$ (MPa)	$P_r$	$T_d$ (°C)	PPTR (kW/TR)	VRC (kJ/m <sup>3</sup> )	CHR (kJ/kg)	$Q_k$ (kW)
R22	0.03656	144.281	39.006	3.698	0	2.2009	0.5870	3.748	96.77	0.950	3217	186.344	6.812
M10	0.03267	161.416	53.780	3.001	-18.84	2.3368	0.4682	4.991	98.76	1.171	2645	225.462	7.367
M20	0.03193	165.176	55.214	2.991	-19.11	2.4342	0.4901	4.966	100.35	1.175	2774	230.708	7.367
M30	0.02952	178.685	54.864	3.256	-11.95	2.0310	0.4032	5.036	96.06	1.079	2499	244.171	7.208
M40	0.02483	212.390	57.132	3.717	0.51	2.0774	0.4998	4.156	84.99	0.945	3072	284.382	7.062
M50	0.02671	197.467	56.385	3.502	-5.30	1.8726	0.4524	4.139	84.70	1.004	2617	268.667	7.176
R407C	0.03623	145.589	49.646	2.932	-20.71	2.5231	0.5311	4.750	96.86	1.199	2869	205.348	7.440

## 6. RESULTS AND DISCUSSION

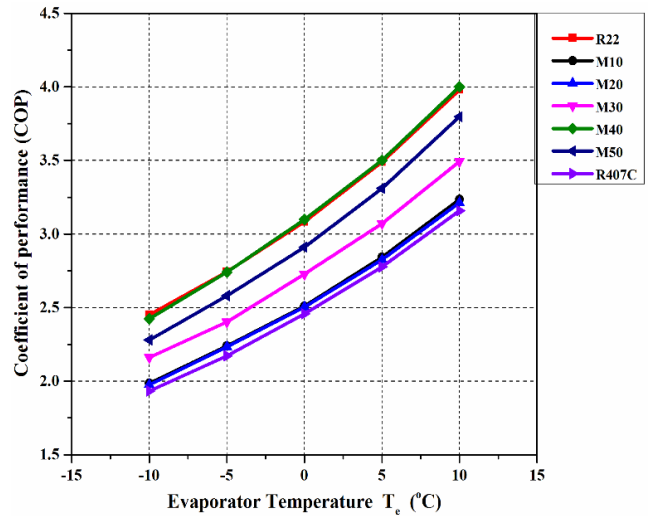
### 6.1 Refrigeration effect

Figure 6. shows the refrigeration effect of R22 and its various alternatives for different evaporator temperatures at

$T_k=54.4^\circ\text{C}$ . From Figure 6, it is observed that the refrigeration effect increases with increase in evaporator temperature for all the investigated refrigerants. The refrigeration effect of both M40 and M50 refrigerants is higher than R22, since latent heat of these refrigerants (M40 and M50) is higher compared to R22.



**Figure 6.** Refrigeration effect of R22 alternatives Vs evaporator temperature



**Figure 8.** COP of R22 alternatives Vs evaporator temperature

### 6.2 Specific work of compressor

Figure 7. shows the specific work of compressor for R22 and its various alternatives for various evaporator temperatures at  $T_k=54.4^\circ\text{C}$ . From Figure 7, it is observed that the work input of compressor decreases with increase in evaporator temperature for all the considered refrigerants. Refrigerants M40 and M50 exhibit higher compressor work compared to R22, since vapour enthalpy values of above refrigerants are higher when compared to R22.

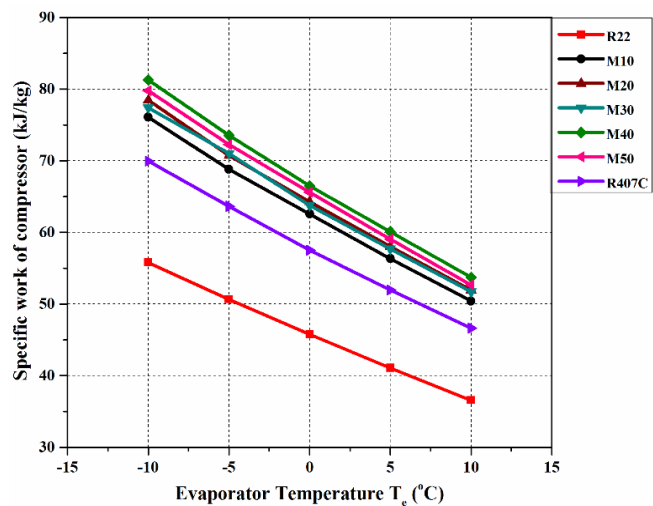


**Figure 7.** Specific work of compressor for R22 alternatives Vs evaporator temperature

### 6.3 Coefficient of performance (COP)

Coefficient of performance can be taken as an index of energy efficiency of the equipment, when it is operating with particular refrigerant. Figure 8. shows the COP of R22 and its different alternatives for various evaporator temperatures at  $T_k=54.4^\circ\text{C}$ . From Figure 8, it is seen that COP of all the refrigerants studied increases as the evaporator temperature rises, since COP depends on both the cooling effect and work of compression. COP of ternary mixture M40 is 0.51% higher, compared to R22 and other investigated refrigerants.

### 6.4 Pressure ratio

Figure 9. shows the pressure ratio of R22 and its various alternatives for various evaporator temperatures at  $T_k=54.4^\circ\text{C}$ . From Figure 9, it is observed that the pressure ratio decreases with increase in evaporator temperature for all the considered refrigerants. This is due to increase in their evaporator pressure with increase in evaporator temperature. Pressure ratio of refrigerants M10, M20 and M30 is higher when compared with R22, since evaporator pressure of these refrigerants is lower when compared to the evaporator pressure of R22. The high pressure ratio causes the increase in discharge temperature of compressor.

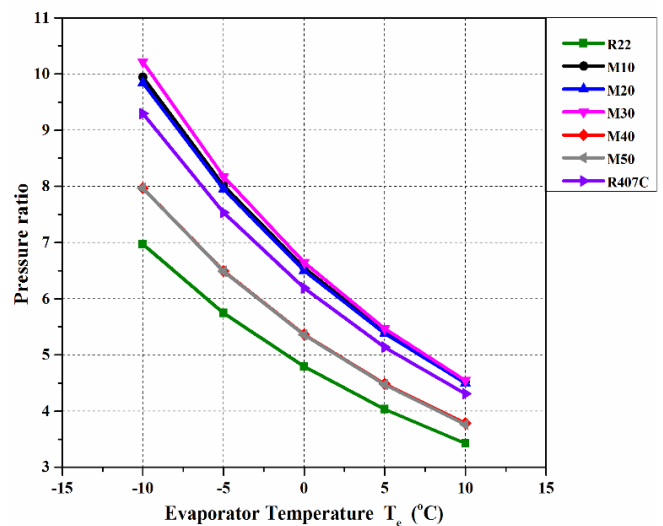


**Figure 9.** Pressure ratio of R22 alternatives Vs evaporator temperature

### 6.5 Compressor discharge temperature

Compressor discharge temperature indicates the life span of the compressor motor. Hence, it is essential to compute the discharge temperature of compressor, operating with various alternative refrigerants. The excessive discharge temperature causes burn out of windings of the compressor motor. Therefore, discharge temperature should be low from the

view point of compressor life. From Figure 10, it is seen that the compressor discharge temperature reduces with rise in evaporator temperature, since pressure ratio of refrigerants decreases with increase in evaporator temperature. Discharge temperatures of both M40 and M50 are lowered by 11.6-11.9°C, compared to R22. Hence, these refrigerants are beneficial from the view point of compressor life. However from Figure 10, it is evident that discharge temperature of refrigerants M10 and M20 increases as evaporator temperature crosses 5°C compared to R22, since pressure ratio of these mixtures (M10 and M20) are higher compared to R22.

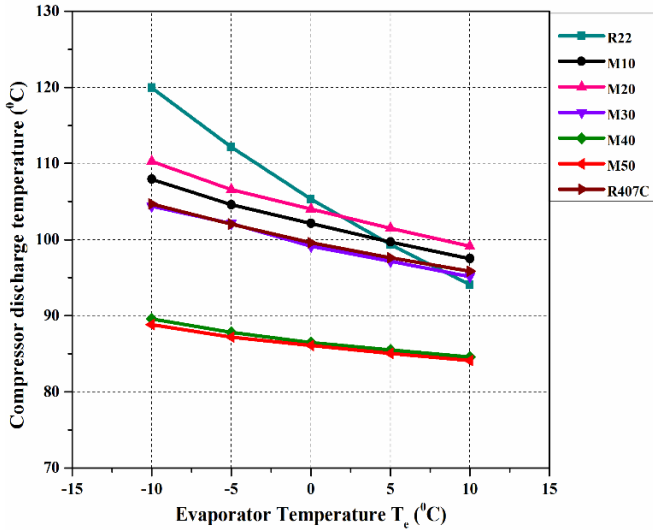


Figure 10. Compressor discharge temperature of R22 alternatives Vs evaporator temperature

### 6.6 Power required per ton of refrigeration

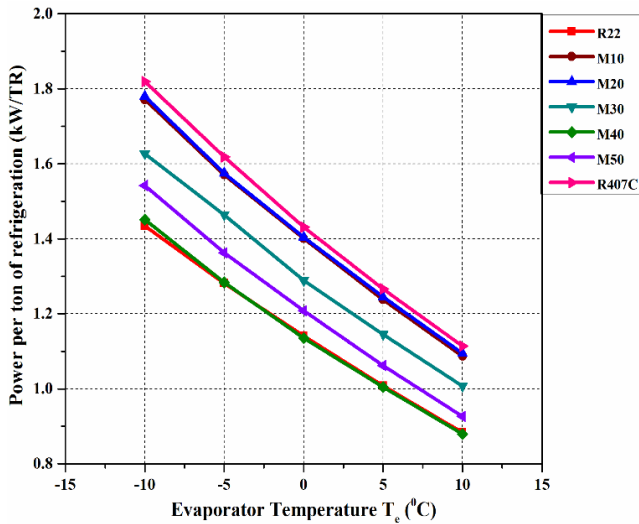


Figure 11. Power per ton of refrigeration of R22 alternatives Vs evaporator temperature

Figure 11. shows the power required per ton of refrigeration of R22 and its various alternatives for different evaporator temperatures at  $T_k=54.4^\circ\text{C}$ . From Figure 11, it is observed that power consumed by the compressor per ton of refrigeration decreases with rise in evaporator temperature for all the considered refrigerants, and this is because of increase in COP with increase in evaporator temperature.

Power consumed per ton of refrigeration of M40 is 0.52% lower compared to R22 and other considered refrigerants.

### 6.7 Volumetric refrigeration capacity

Figure 12. shows the volumetric refrigeration capacity of various R22 alternatives for different evaporator temperatures at  $T_k=54.4^\circ\text{C}$ . Volumetric capacity depends upon the vapour density occurs at the outlet of evaporator and also on the refrigeration effect. From Figure 12, it is observed that volumetric refrigeration capacity increases with increase in evaporator temperature for all the studied refrigerants, since volumetric refrigeration capacity depends on both the values of vapour density at exit of evaporator and refrigeration effect of the refrigerants. Volumetric refrigeration capacity of M40 refrigerant is the highest among the five studied refrigerants and it is closer to that of R22. Therefore, the same R22 compressor can be used for M40, when compared to other refrigerants.

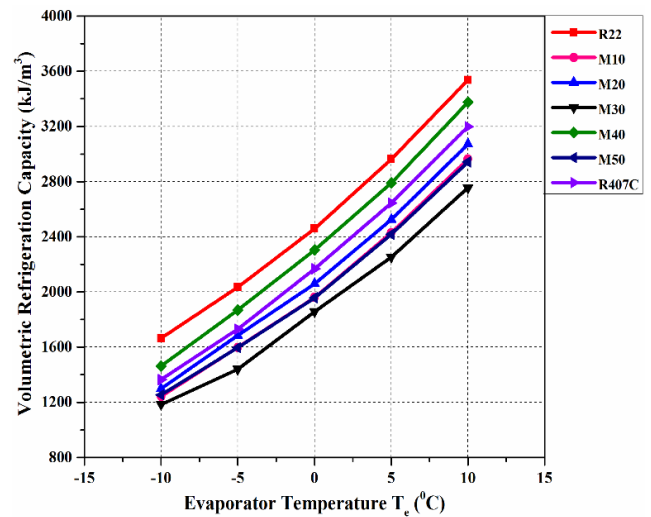


Figure 12. Volumetric refrigeration capacity of R22 alternatives Vs evaporator temperature

### 6.8 Condenser heat rejection

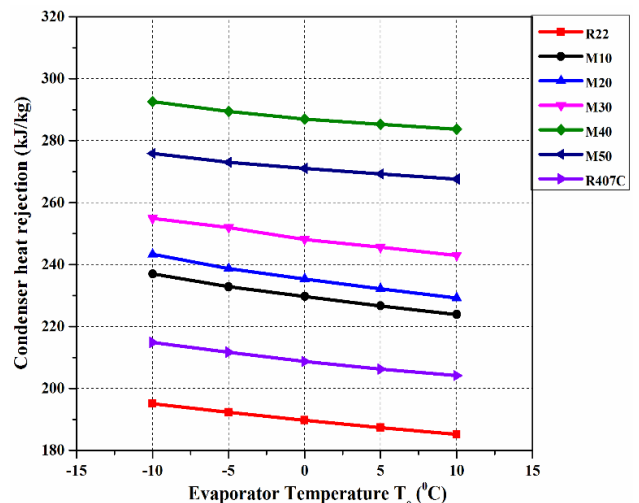


Figure 13. Condenser heat rejection of R22 alternatives Vs evaporator temperature

Figure 13. shows the condenser heat rejection of various

R22 alternatives for different evaporator temperatures at  $T_k=54.4^{\circ}\text{C}$ . From Figure 13, it is observed that condenser heat rejection decreases with increase in evaporator temperature, because latent heat of condensation of refrigerants decreases with increase in evaporator temperature. Condenser heat rejection of both M40 and M50 is higher than R22, since these refrigerants are blended with hydrocarbons, which will have high latent heat of condensation compared to R22.

### 6.9 Heat transfer through condenser

Figure 14. shows the heat transfer through the condenser of R22 alternatives for various evaporator temperatures at  $T_k=54.4^{\circ}\text{C}$ . Heat transfer through condenser indicates the load taken by the condenser to reject heat for the given fluid. It depends on mass flow rate and latent heat of condensation of the refrigerants. From Figure 14, it is observed that heat transfer through condenser, decreases with rise in evaporator temperature. And also, from Figure 14, it is evident that heat transfer through condenser, for R407C, is higher than R22 and the other five investigated refrigerants. This is because of net effect of mass flow rate and latent heat of condensation of R407C, compared to R22 and the other five investigated refrigerants.

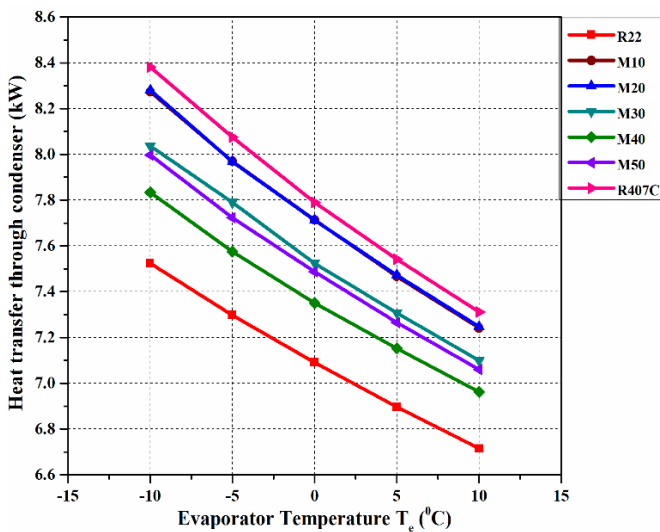


Figure 14. Heat transfer through condenser of R22 alternatives Vs evaporator temperature

### 7. CONCLUSIONS

From the thermodynamic Performance as well as from Refrigerant Flammability (RF) number analysis of various investigated R22 alternative refrigerants, the conclusions can be drawn as follows.

(i) COP of M40 was 0.51% higher compared to R22 and the other refrigerants studied.

(ii) Compressor discharge temperatures of both M40 and M50 refrigerants were lowered by 11.6-11.9 $^{\circ}\text{C}$  compared to R22. Hence, both the refrigerants exhibit better durability of the compressor motor windings. Similarly GWP<sub>100</sub> of both M40 (815) and M50 (815) refrigerants was lower compared to that of GWP<sub>100</sub> of R22 (1760).

(iii) Power consumed per ton of refrigeration of M40 was 0.52% lower compared to R22 and the other refrigerants

studied.

(iv) Volumetric refrigeration capacity of M40 was very close to that of R22. Therefore, similar R22 compressor could be used for M40.

(v) Heat transfer through the condenser for R407C was higher, compared to R22 and the other five blends studied.

(vi) RF analysis revealed that refrigerant blends (M10 to M50) were categorized into weakly flammable refrigerants (ASHRAE A2 category), since RF number of these refrigerants was less than 30 kJ/g.

(vii) Overall, thermodynamic performance of new ternary refrigerant mixture M40 (R32/R134a/R1270 5/60/35 by mass %) was better than that of R22 from the stand point of COP, discharge temperature, GWP and power savings. Therefore, refrigerant M40 could be an eco-friendly alternative to R22 used in residential air conditioners.

### REFERENCES

- [1] United Nations Environmental Programme. (1987). Montreal Protocol on substances that deplete the ozone layer Final act. New York, United Nations.
- [2] Powell RL. (2002). CFC Phase out; have we met the challenge. *Journal of Fluorine Chemistry* 114(2): 237-250. [https://doi.org/10.1016/S0022-1139\(02\)00030-1](https://doi.org/10.1016/S0022-1139(02)00030-1)
- [3] Devotta S, Waghmare AV, Sawant NN, Domkundwar BM. (2001). Alternatives to HCFC-22 for air conditioners. *Applied Thermal Engineering* 21(6): 703-715. [https://doi.org/10.1016/S1359-4311\(00\)00079-X](https://doi.org/10.1016/S1359-4311(00)00079-X)
- [4] Maczek K, Muller J, Wojtas K, Domanski PA. (1997). Ternary zeotropic mixture with CO<sub>2</sub> component for R22 heat pump application. CLIMA conference, Brussels, Belgium, pp. 1-9.
- [5] Han XH, Wang Q, Zhu ZW, Chen GM. (2007). Cycle performance study on R32/R125/R161 as an alternative refrigerant to R407C. *Applied Thermal Engineering* 27(14-15): 2559-2565. <https://doi.org/10.1016/j.applthermaleng.2007.01.034>
- [6] Yildirim C, Ozkan DB, Onan C. (2016). Theoretical study of R32 to replace R410A in variable refrigerant flow systems. *International Journal of Ambient Energy* 39(1): 87-92. <https://doi.org/10.1080/01430750.2016.1269682>
- [7] Jung D, Song Y, Park B. (2000). Performance of HCFC22 alternative refrigerants. *International Journal of Refrigeration* 23(6): 466-474. [https://doi.org/10.1016/S0140-7007\(99\)00066-3](https://doi.org/10.1016/S0140-7007(99)00066-3)
- [8] Park KJ, Jung D. (2007). Thermodynamic performance of HCFC22 alternative refrigerants for residential air-conditioning applications. *Energy and Buildings* 39(6): 675-680. <https://doi.org/10.1016/j.enbuild.2006.10.003>
- [9] Bolaji BO. (2011). Performance investigation of ozone-friendly R404A and R507 refrigerants as alternatives to R22 in a window air-conditioner. *Energy and Buildings* 43(11): 3139-3143. <https://doi.org/10.1016/j.enbuild.2011.08.011>
- [10] Park KJ, Shim YB, Jung D. (2009). A drop-in refrigerant R431A for replacing HCFC22 in residential air-conditioners and heat pumps. *Energy Conversion and Management* 50(7): 1671-1675. <https://doi.org/10.1016/j.enconman.2009.03.027>
- [11] Aprea C, Mastrullo R, Renno C, Vanoli GP. (2004). An evaluation of R22 substitutes performances regulating

- continuously the compressor refrigeration capacity. *Applied Thermal Engineering* 24(1): 127-139. [https://doi.org/10.1016/S1359-4311\(03\)00187-X](https://doi.org/10.1016/S1359-4311(03)00187-X)
- [12] Chang YS, Kim MS, Ro ST. (2000). Performance and heat transfer characteristics of hydrocarbon refrigerants in a heat pump system. *International Journal of Refrigeration* 23(3): 232-242. [https://doi.org/10.1016/S0140-7007\(99\)00042-0](https://doi.org/10.1016/S0140-7007(99)00042-0)
- [13] Martin JJ, Hou YC. (1955). Development of an equation of state for gases. *AIChE Journal* 1(2): 142-151. <https://doi.org/10.1002/aic.690010203>
- [14] De Monte F. (2002). Calculation of thermodynamic properties of R407C and R410A by the Martin–Hou equation of state - part I: Theoretical development. *International Journal of Refrigeration* 25(3): 306-313. [https://doi.org/10.1016/S0140-7007\(01\)00028-7](https://doi.org/10.1016/S0140-7007(01)00028-7)
- [15] De Monte F. (2002). Calculation of thermodynamic properties of R407C and R410A by the Martin–Hou equation of state - part II: technical interpretation. *International Journal of Refrigeration* 25(3): 314-329. [https://doi.org/10.1016/S0140-7007\(01\)00029-9](https://doi.org/10.1016/S0140-7007(01)00029-9)
- [16] ASHRAE. (2009). Handbook fundamentals (SI). Chapter 29, Refrigerants, pp. 29.1-29.10.
- [17] Arora CP. (2009). Refrigeration and air conditioning. tata McGraw-Hill, New Delhi.
- [18] Poling BE, Prausnitz JM, John P, O’Connell. (2001). The properties of gases and liquids. McGraw-Hill, New York.
- [19] Forero GLA, Velásquez JJA. (2011). Wagner liquid-vapour pressure equation constants from a simple methodology. *The Journal of Chemical Thermodynamics* 43(8): 1235-1251. <https://doi.org/10.1016/j.jct.2011.03.011>
- [20] Reid RC, Prausnitz JM, Sherwood TK. (1977). The properties of gases and liquids. McGraw-Hill, New York.
- [21] Nasrifar K, Moshfeghian M. (1999). Evaluation of saturated liquid density prediction methods for pure refrigerants. *Fluid Phase Equilibria* 158: 437-445. [https://doi.org/10.1016/S0378-3812\(99\)00068-0](https://doi.org/10.1016/S0378-3812(99)00068-0)
- [22] Chueh PL, Prausnitz JM. (1967). Third virial coefficients of nonpolar gases and their mixtures. *AIChE Journal* 13: 896-902. <https://doi.org/10.1002/aic.690130516>
- [23] ANSI/ASHRAE for Designation and Safety Classification of Refrigerants (2007). ANSI/ASHRAE Standard 34.
- [24] Kondo S, Takahashi A, Tokuhashi K, Sekiya A. (2002). RF number as a new index for assessing combustion hazard of flammable gases. *Journal of Hazardous Materials* 93(3): 259-267. [https://doi.org/10.1016/S0304-3894\(02\)00117-6](https://doi.org/10.1016/S0304-3894(02)00117-6)
- [25] Chen J, Yu J. (2008). Performance of a new refrigeration cycle using refrigerant mixture R32/R134a for residential air-conditioner applications. *Energy and Buildings* 40(11): 2022-2027. <https://doi.org/10.1016/j.enbuild.2008.05.003>
- [26] Dalkilic AS, Wongwises S. (2010). A performance comparison of vapour-compression refrigeration system using various alternative refrigerants. *International Communications in Heat Mass Transfer* 37(9): 1340–1349. <https://doi.org/10.1016/j.icheatmasstransfer.2010.07.006>
- [27] Bolaji BO, Huan Z. (2012). Computational analysis of the performance of ozone-friendly R22 alternative refrigerants in vapour compression. *Air-Conditioning Environment Protection Engineering* 38(4): 41-52. <https://doi.org/10.5277/EPE120404>
- [28] Bolaji BO, Huan Z. (2014). Performance investigation of some hydro-fluorocarbon refrigerants with low global warming as substitutes to R134a in refrigeration systems. *Journal of Engineering Thermophysics* 23(2): 148-157. <https://doi.org/10.1134/S1810232814020076>
- [29] Babu TP, Samaje VV, Rajeev R. (2006). Development of Zero ODP, Less TEWI, Binary, Ternary and Quaternary Mixtures to Replace HCFC-22 in Window Air-Conditioner. *International Refrigeration and Air Conditioning Conference, Purdue, USA*, pp. 1-8.
- [30] Tian Q, Cai D, Ren L, Tang W, Xie Y, He G, Liu F. (2015). An experimental investigation of refrigerant mixture R32/R290 as drop-in replacement for HFC410A in household air conditioners. *International Journal of Refrigeration* 57: 216-228. <https://doi.org/10.1016/j.ijrefrig.2015.05.005>

## NOMENCLATURE

BP	Boiling point, °C
COP	Coefficient of performance, Dimensionless
CHR	Condenser heat rejection, kJ/kg
LFL	Lower flammability limit, kg/m <sup>3</sup>
MW	Molecular weight, kg/kmol
PPTR	Power required per ton of refrigeration, kW/TR
RE	Refrigeration effect, kJ/kg
TR	Ton of refrigeration, kW
UFL	Upper flammability limit, kg/m <sup>3</sup>
VRC	Volumetric refrigeration capacity, kJ/m <sup>3</sup>
C <sub>p0</sub>	Ideal heat capacity, J/mol K
h	Enthalpy, kJ/kg
h <sub>f</sub>	Liquid enthalpy, kJ/kg
h <sub>fg</sub>	Enthalpy of vapourization, kJ/kg
h <sub>g</sub>	Vapour enthalpy, kJ/kg
h <sub>1g</sub>	Enthalpy at evaporator outlet, kJ/kg
h <sub>1</sub>	Enthalpy at compressor inlet, kJ/kg
h <sub>2</sub>	Enthalpy at compressor outlet, kJ/kg
h <sub>2f</sub>	Enthalpy at condenser inlet, kJ/kg
h <sub>3e</sub>	Enthalpy at condenser outlet, kJ/kg
h <sub>4</sub>	Enthalpy at evaporator inlet, kJ/kg
h <sub>1''</sub>	Enthalpy at compressor inlet, kJ/kg
h <sub>2''</sub>	Enthalpy at compressor outlet, kJ/kg
h <sub>3''</sub>	Enthalpy at condenser outlet, kJ/kg
h <sub>4''</sub>	Enthalpy at evaporator inlet, kJ/kg
P	Pressure, MPa
P <sub>c</sub>	Critical pressure, Mpa
P <sub>cm</sub>	Critical pressure of mixture, MPa
P <sub>e</sub>	Evaporating pressure, MPa
P <sub>k</sub>	Condensing pressure, MPa
P <sub>r</sub>	Pressure ratio, Dimensionless
P <sub>sat</sub>	Saturation pressure, MPa
q	Enthalpy of combustion, kJ/mol
Q <sub>c</sub>	Refrigeration capacity, kW
Q <sub>k</sub>	Heat transfer through condenser, kW
R	Universal gas constant, J/mol K
S <sub>f</sub>	Liquid entropy, kJ/kg K
S <sub>fg</sub>	Entropy of vapourization, kJ/kg K
S <sub>g</sub>	Vapour entropy, kJ/kg K

T	Temperature, K
T <sub>bub</sub>	Bubble point temperature, °C
T <sub>c</sub>	Critical temperature, K
T <sub>cm</sub>	Critical temperature of mixture, K
T <sub>dew</sub>	Dew point temperature, °C
T <sub>e</sub>	Evaporating temperature, °C
T <sub>glide</sub>	Temperature glide, °C
T <sub>k</sub>	Condensing temperature, °C
T <sub>sat</sub>	Saturation temperature, K
U	Internal energy, kJ/kg
V	Specific volume, m <sup>3</sup> /kg
V <sub>cm</sub>	Critical volume of mixture, m <sup>3</sup> /kg
V <sub>g</sub>	Vapour volume, m <sup>3</sup> /kg
V <sub>f</sub>	Liquid volume, m <sup>3</sup> /kg
W <sub>c</sub>	Specific work of compressor, kJ/kg
W <sub>cp</sub>	Compressor power, W
Z <sub>cm</sub>	Critical compressability factor of mixture, Dimensionless
ρ	Density, kg/m <sup>3</sup>
ρ <sub>c</sub>	Critical density, kg/m <sup>3</sup>
ω	Acentric factor, Dimensionless

### Greek symbols

ρ	Density, kg/m <sup>3</sup>
ω	Acentric factor, Dimensionless

### Subscripts

c	Critical
f	Liquid phase
g	Vapour phase
m	Mixture

### Abbreviations

AHRI	Air-Conditioning, Heating, and Refrigeration Institute
ASHRAE	American Society of Heating, Refrigerating and Air-Conditioning Engineers
BP	Boiling point
CHR	Condenser heat rejection
COP	Coefficient of performance
GWP	Global warming potential
HCFCs	Hydrochlorofluorocarbons
ODP	Ozone depleting potential
PPTR	Power required per ton of refrigeration
RE	Refrigeration effect
RF	Refrigerant flammability
TR	Ton of refrigeration
VCR	Vapour compression refrigeration
VRC	Volumetric refrigeration capacity